

Study of the white light and hard X-rays emission of the M6.6 class flare of February 18 2011 using SDO/HMI and RHESSI

Juan Sebastián Castellanos-Durán¹, Julian David Alvarado-Gómez¹, J.C. Martínez Oliveros² and Benjamin Calvo-Mozo¹



¹Group of Solar Astrophysics, Observatorio Astronómico Nacional, Universidad Nacional de Colombia.
²Space sciences laboratory, UC Berkeley.
 Contact: jscastellanosd@unal.edu.co

Abstract

Solar flares are sudden release energy that occur on the upper layers of solar atmosphere (corona). They influence the others layers of the solar atmosphere and the interplanetary space. We present a characterization of the solar event (SOL2011-02-18T10:11) GOES M6.6, hosted by the active region NOAA 11158, studying the correlation between the white light emission, hard and soft X-rays. We estimate the ratio between collisional electronic densities and the trapped in the magnetic mirror electronic densities, finding that the number of particles which propagating to the photosphere during the flare was ≈ 1.55 times greater than number particles confined in the loop using data from SDO/HMI and RHESSI.

Theoretical Background

✧ Hard X-ray emission

The *Bremsstrahlung* emission can be divided in three classes (i) thermal, (ii) thick-target and (iii) thin-target. For our considerations the emission in this wavelength regime is dominated by thick-target bremsstrahlung which consists of electrons accelerated in a Coulomb electric field that are scattered by other charged particles. In a quasi-elastic approximation this can be expressed with the Rutherford cross section. The hard X-ray intensity is given by

$$I(\epsilon_x) = \frac{1}{4\pi R^2} \int_{\epsilon_x}^{\infty} \sigma(\epsilon, \epsilon) v(\epsilon) \left(\int n_p n_e(\epsilon) dV \right) d\epsilon \quad (1)$$

where $\sigma(\epsilon, \epsilon)$ is the cross section.

✧ White light emission

In this radiation, the chromospheric and photospheric plasma are heated, producing an increase in pressure leading to: (i) chromospheric evaporation, (ii) local temperature increases leading to the generation of white light emission, that back body radiation given by the Planck's law. This can be an approximation to a

$$I(\nu, T) = \frac{2h}{c^2} \frac{\nu^3}{\exp\left(\frac{h\nu}{k_B T}\right) - 1} \quad (2)$$

✧ Soft X-ray and extreme ultraviolet emission

After the reconnection charged particles are injected to the loop, and their movement is given by the magnetic field shape, in which is very strong near to the footpoints and is lower in the higher height. This gradient produce that the charged particles trapped and start to emitted in a soft X-rays and extreme ultraviolet emission; this is called mirror magnetic effect. The pitch angle which needs the particles to get trapping (α_0) needs to be greater than

$$\alpha_0 < \sin^{-1} \sqrt{\frac{1}{R}}, \quad R = \frac{B_{top}}{B_0} \quad (3)$$

where R is the magnetic mirror radius.

Observations

The solar flare SOL2011-02-18T10:11 was hosted in the active region NOAA 11158 with heliocentric coordinates 19S - 59W and started 10:06:44UT, reaching its maximum in soft X-rays at 10:10:22UT and ended at 10:16:36UT.

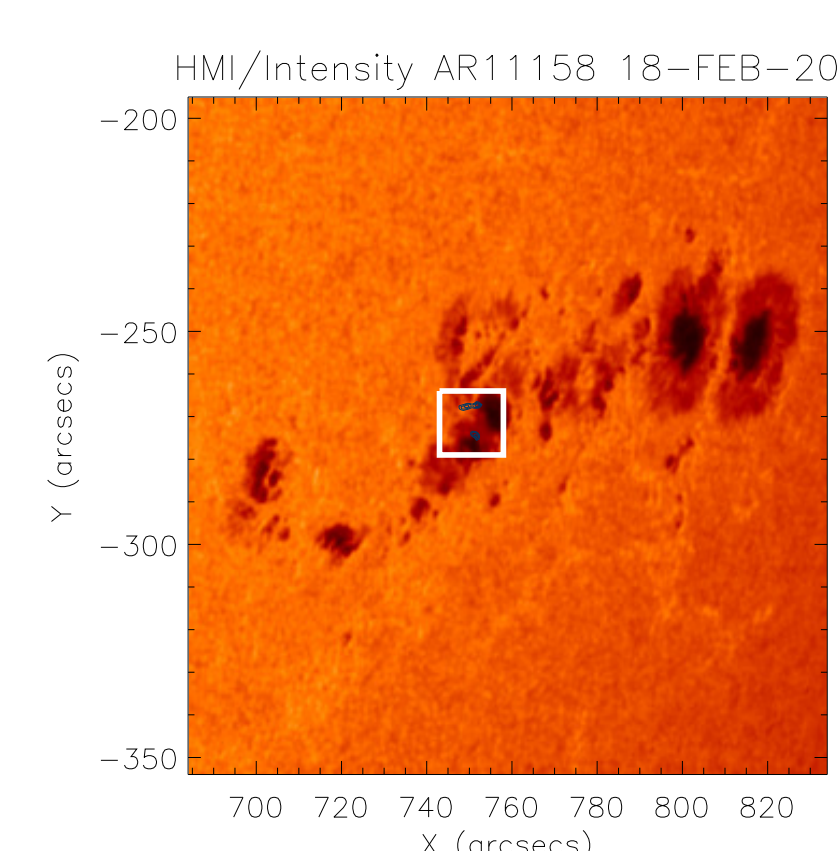


Fig 1: The NOAA AR 11158 in February 18 of 2012 was the place where M6.6 GOES class took place. Over it contour plots with levels 60, 70, 80, 90 % of the maximum detected in white light intensity taken by SDO/HMI.

Flare Emission

Fig. 2 show the three physical observations taken by SDO/HMI and the differences in the continuum emission. The lower panels (e and f) show the RHESSI contours with energy bands 12-25 keV, 30-80 keV and 25-50 keV over the consecutive intensity differences maps.

The fig 2(d) shows footpoints areas of ($\approx 2.12\text{Mm}^2$ and $\approx 0.90\text{Mm}^2$). Compared to the total AR-area $\approx 2,83\text{Gm}^2$, the emission kernels were about 0.1% of the total area, while the white light transient intensity was 25% higher than the background.

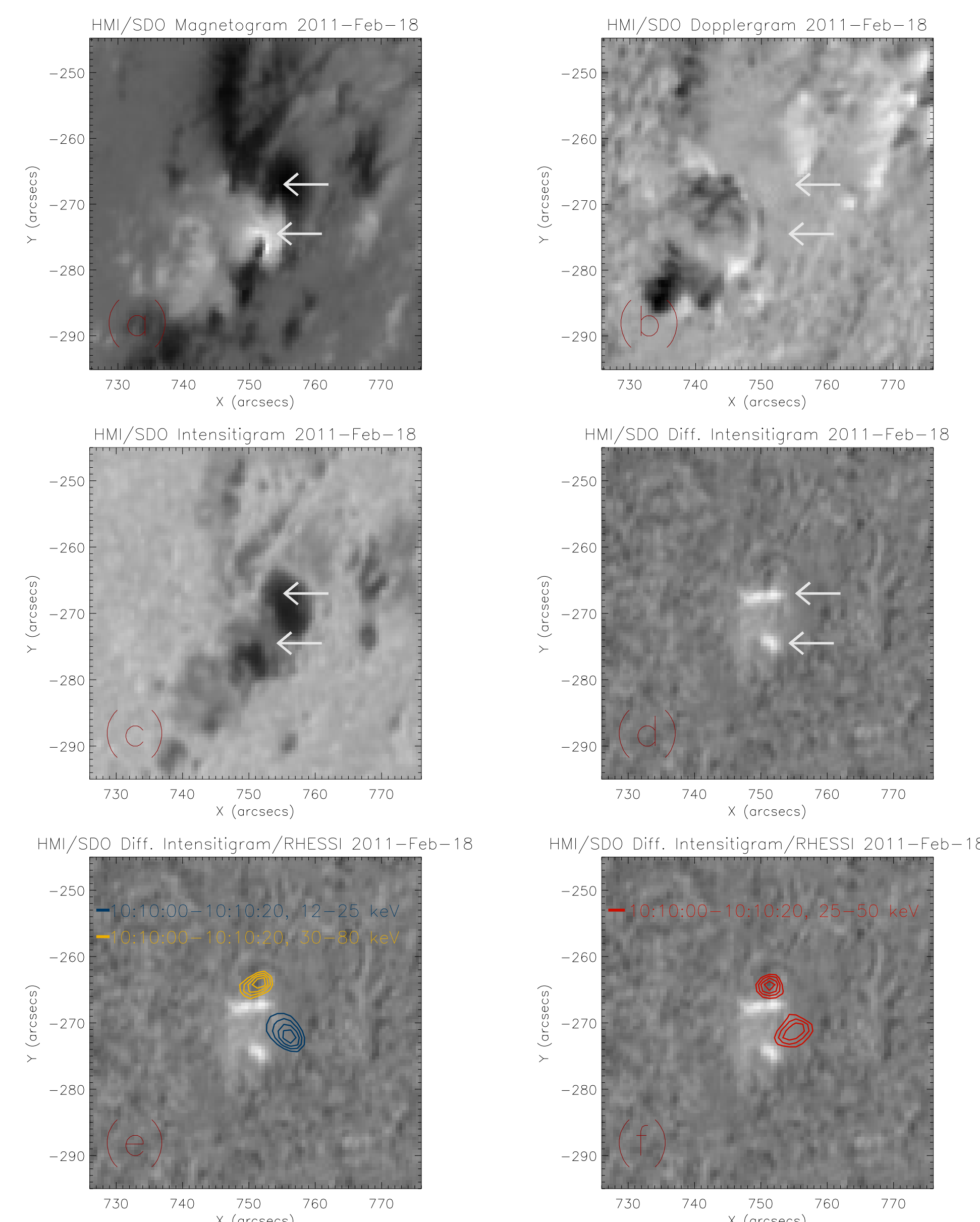


Fig 2: The images (a), (b), (c) are the magnetogram, dopplergram and intensity of continuum emission (respectively) taken by SDO/HMI at the maximum of the M6.6 flare. Panel (d) is the difference in intensity and panels (e) and (f) also have the overplotted RHESSI contours using the CLEAN algorithm, with 60, 70, 80, 90% of the emission. The white arrows are pointing to the WL emission kernels.

Figures 2 (f,g) show the spatial correlation between the white light and the HXR emission kernels. The blue RHESSI contours at the northern footpoint (12-25 keV band) are assumed to be the main source of the SXR, while the other kernel (southern yellow contours) is likely to be the source of HXR (30-80 keV band). The middle energy band (25-50 keV), represented by the red contours, is used to show that both sources have a mixed population and their time is slightly different. Then, our assumption may not be completely accurate.

Reference

- Fletcher and h. S. Hudson, "Spectral and spatial variations of flare hard X-ray footpoints." *Solar Physics* 210, pp 307-321, 2002.
- J. Aschwanden, "Particle acceleration and kinematics in solar flares." Chapter 8, pp 157-160.
- M. Aschwanden, "Physics of the solar corona. An introduction with problems and solutions". Chapter 12. pp 537-539.
- A. O. Benz, "Flare Observations". *Living Reviews in Solar Physics* 2007.
- J.C. Martínez Oliveros et al, "The height of a white-light flare and its hard X-ray sources"

White Light and HXR Radiation

We made the assumption that the ratio of the HXR (F_{HXR}) and the SXR (F_{SXR}) fluxes is proportional to the white light flux, in the locality where the HXR were emitted (F_{WL}^{HXR}), and the white light flux, where the SXR were emitted (F_{WL}^{SXR})

$$\frac{F_{HXR}}{F_{SXR}} \propto \frac{F_{WL}^{HXR}}{F_{WL}^{SXR}} \quad (4)$$

The Fig. 3 shows the white light curve in both footpoints and we calculate the peak and emission flux (Tab. 1)

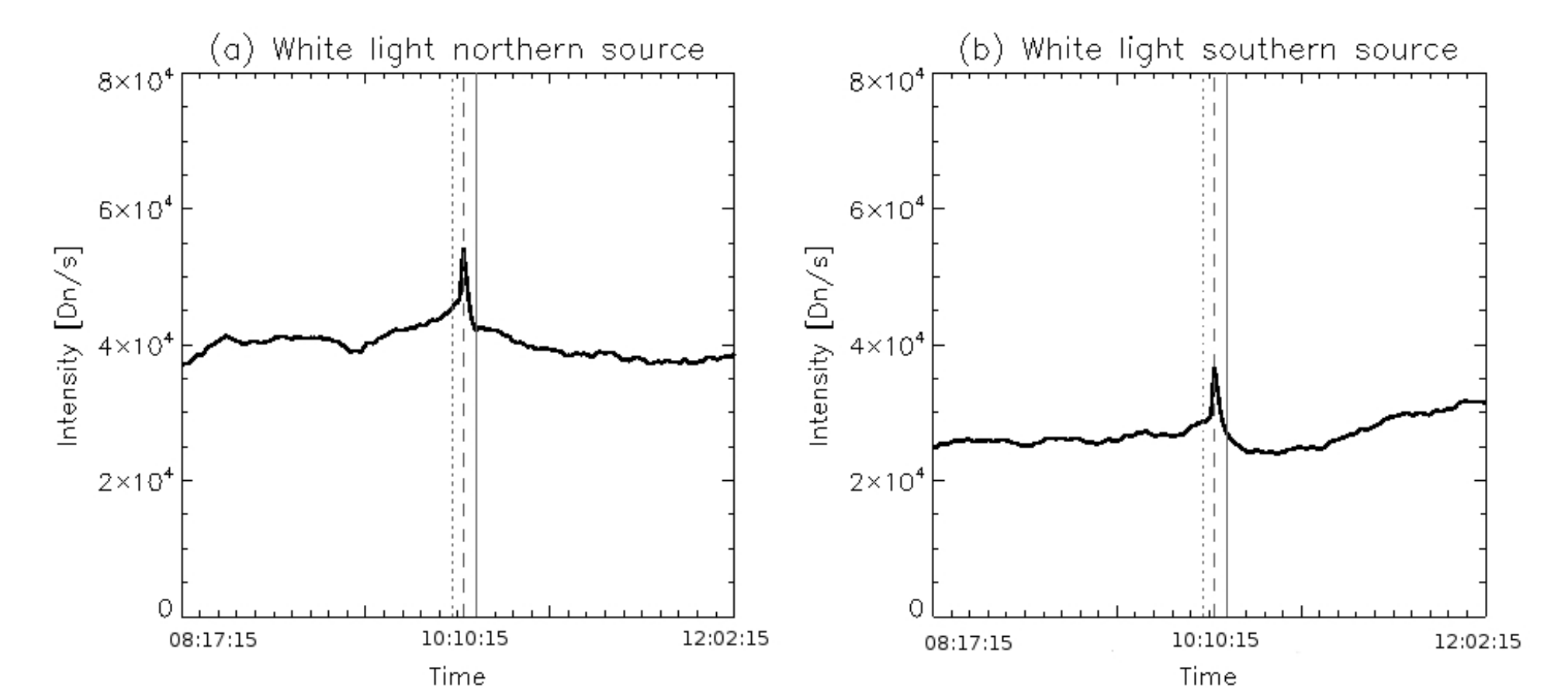


Fig 4: White light curve at the emission kernels during three hours centered at the peak of the flare in SXR.

	Northern source	Southern source
WL peak [Dn/s]	5.43×10^4	3.67×10^4
WL flux [Dn]	9.24×10^5	5.95×10^5
Rate	1.48	1.55

Tab 1: Flux and peak of the white light emission in both kernels.

The next relation tell us the ratio between the electron density trapped in the magnetic mirror (ρ_{pre}) and the electron density of the electrons due to the thick target (ρ_{loop}) emitting in hard X-rays

$$\frac{\rho_{pre}}{\rho_{loop}} \approx 3/2 \quad (5)$$

Magnetic Field Variation

We estimated the change of the magnetic field along the line-of-sight B_{los} over the region where the white-light emission was observed. At the northern source, we divided the time interval by pre-flare (green), during flare (red) and post-flare (yellow) and we fitted three different linear behaviors, obtaining the the slopes before and after the flare were similar $\Delta B_{bef}/\Delta t \approx -7,12 \text{ G/s}$ and $\Delta B_{aft}/\Delta t \approx -7,55 \text{ G/s}$ and during the flare the slope was $\Delta B_{aft}/\Delta t \approx -9,55 \text{ G/s}$.

The southern source showed a different behavior because the magnetic field is stronger than in the other one, and the total rate of change in the line-of-sight field was estimated as $\Delta B_{bef-aft}/\Delta t \approx -3,61 \text{ G/s}$.

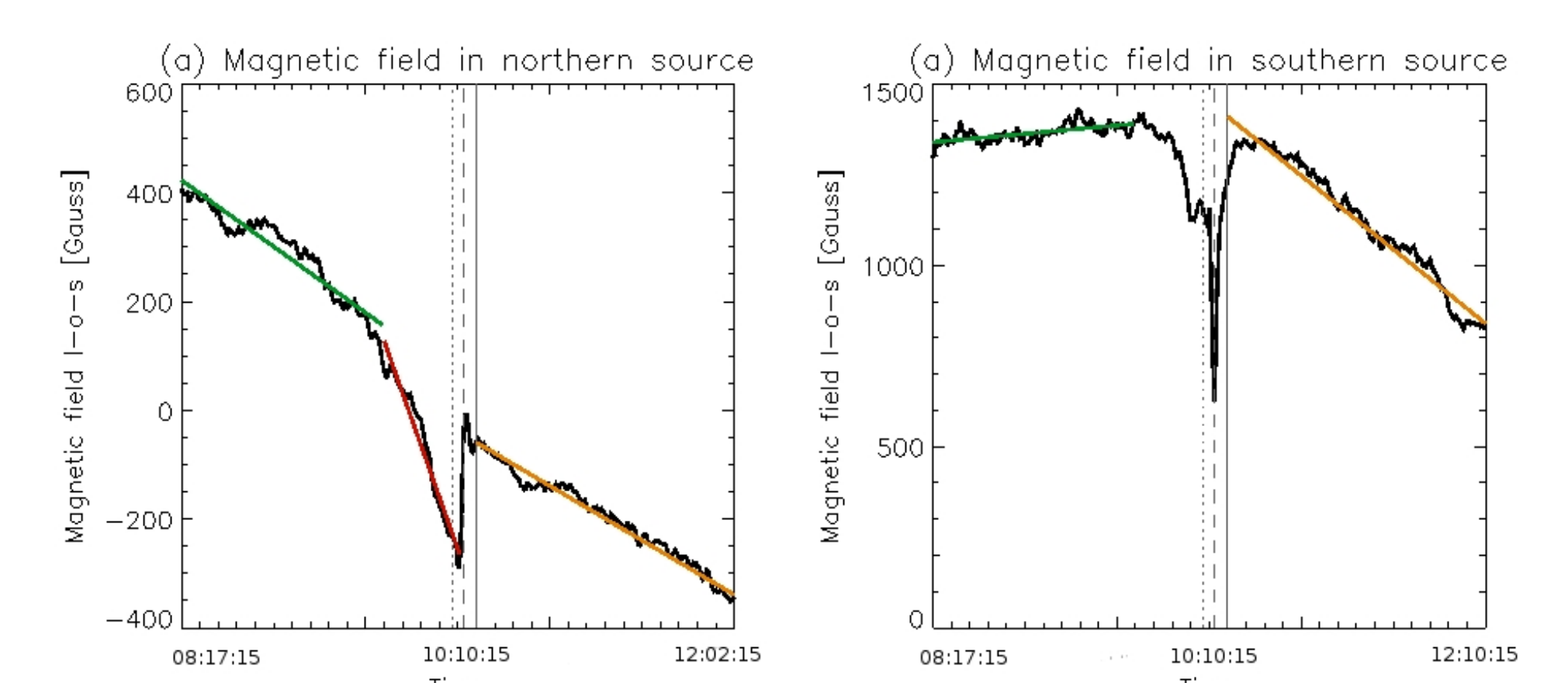


Fig 3: The line-of-sight magnetic field transient, integrated over the WL-kernels location, during a time interval of three hours centered at the maximum of the M6.6 flare.